Journal of Physics and Its Applications

Journal homepage : https://ejournal2.undip.ac.id/index.php/jpa/index

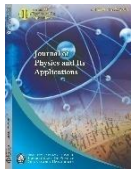

Developing 1-D velocity model along Matano Fault Zone, Sulawesi, Indonesia

Madona[1,2], M.S. Rosid[1*], D. Handoko[1], and D.S.J. Sianipar[2]

[1]*Physics Department, FMIPA Universitas Indonesia, Depok, Indonesia*
[2]*The Agency for Meteorology, Climatology, and Geophysics, Jakarta, Indonesia*

[*]*Corresponding author : syamsu.rosid@ui.ac.id*

ARTICLE INFO

Article history:
Received: 28 October 2025
Accepted: 5 December 2025
Available online: 27 February 2026

Keywords:
Matano
Velocity Model
Velest

ABSTRACT

The Matano Fault, with a slip rate of ~ 20 mm/year, is the most active strike-slip fault in Sulawesi after the Palu-Koro Fault. As a result, this region exhibits a high level of seismicity. Unfortunately, a number of studies that have been conducted only involve a less dense network of stations and global velocity models. This study aims to obtain an optimum velocity model using the VELEST program, which reliably represents the actual condition of the study area. The data used in this study consists of hypocenter, origin times, and P-wave arrival times from earthquakes (Mw ≥ 3), each containing at least six clearly identified P-wave phases. These data were obtained from 317 events that occurred within the region bounded by 120.10°E – 122.20°E and 2.99°S – 1.66°S during the period from January 2022 to March 2025. To determine the optimum 1-D velocity model, four initial models were tested, namely Koulakov, Arimuko, Crust, and Bunaga. These models were evaluated based on RMS, the stability test of the updated velocity model, uncertainty assessment using bootstrap test, and their consistency with previous studies. The evaluation results indicate that the Arimuko Model is the most reliable, as it provides the lowest RMS value, stable hypocenter relocations (±6–7 km), bootstrap results showing narrow uncertainty intervals, and consistency with earlier studies that identified a low-velocity zone. The result of this study is expected to serve as a reference for earthquake relocation and seismicity analysis at the Matano Fault Zone.

1. Introduction

The Matano Fault is a strike slip fault characterized by steep cliff morphology, with fault planes dipping at angles ranging from approximately 75° to 90°. The fault extends for about 190 km from the southeastern coast of Sulawesi, passing through Lake Matano and terminating at its junction with the Palu Koro Fault [1, 2, 3]. With an east southeast to northwest orientation, this fault is one of the most active in Sulawesi after the Palu Koro Fault, exhibiting a slip rate of about 20 mm per year [4, 5, 6]. These conditions result in high seismic activity in the surrounding region. Several events have been identified as significant earthquakes around Matano Fault, including the 2011 Mw 6.1 Sorowako [7], 1961 Mw 6.0 Matano [8], and 1954 Mw 6.0 Matano [9]. Particulary, the 2011 event caused severe damage such as the collapse of 18 houses and the destruction of a community health center and a mosque in Towuti District [10, 11, 12]. This phenomenon confirms that the Matano Fault poses a significant seismic hazard to the surrounding communities.

Based on digital remote sensing imagery and direct field [2, 6], the fault system comprises six distinct segments: Kuleana, Pewusai, Matano, Pamsoa, Ballawai, and Geresa. Geomorphologically, these segments are generally characterized by high, steep scarps resulting from tectonic displacement, as well as narrow valleys [1, 9].

The Matano lies within the Sulawesi Ophiolite Complex, a geological formation characterized by mafic and ultramafic rocks, superimposed by capping limestone. This complex, recognized globally as the third largest ophiolite belt after those in Oman and Papua New Guinea, is rich in economic minerals derived from its host rocks. Specifically, the eastern section of the Matano Fault contains significant deposits of nickel and iron. Consequently, this region holds high strategic value for mineral extraction exemplified by the long-standing nickel exploration and mining operations conducted by PT Vale Indonesia Tbk in Sorowako, South Sulawesi, since 1968 [13]. However, locating mining operations on an active fault poses serious risks, making earthquake hazard mitigation essential.

Some studies have been conducted to identify the characteristics and activity of the Matano Fault through various scientific approaches, including paleoseismic methods, focal mechanism analyses, b-value and a-value calculations, and GNSS or GPS based geodetic analyses [14, 15]. These studies have made important contributions to understanding the morphology, slip rate, and tectonic dynamics along the Matano Fault. However, research that specifically

focuses on the seismicity aspect remains relatively limited.

One of the studies related to seismicity, namely the earthquake relocation analysis around the Matano Fault, has been conducted previously. However, this research was limited to the use of a global velocity model [16]. Efforts to relocate earthquakes around the Matano Fault using a local velocity model have also been carried out [17, 18], but the velocity model was developed using earthquake data from the 2009–2018 period, when the distribution of seismic stations across Sulawesi was still sparse and only a few stations had been installed in Central Sulawesi (Fig. 1). In addition, the results of the velocity modeling indicated signs of overfitting due to an excessive number of iterations (non-optimum), as reflected by the insignificant decrease in RMS values. Therefore, the relocation results obtained from previous studies have not yet been able to accurately represent the hypocenter distribution in the area surrounding the Matano Fault. This condition highlights the need to develop a more representative velocity model by utilizing recent seismic data and a more evenly distributed station network, so that earthquake relocation results can better characterize the seismicity patterns [19] and subsurface structure in the region.

A velocity model for Sulawesi has also been developed using the Ambient Noise Tomography (ANT) method [20]. Unfortunately, the study area coverage is too broad, covering both Kalimantan and Sulawesi, resulting in a model resolution that is insufficiently detailed to capture local velocity variations across Sulawesi. Moreover, the modeling results obtained from this method strongly depend on the quality of the ambient seismic noise signals, such as those generated by ocean waves, wind, or human activities [21]. If the noise sources are weak or unevenly distributed, the interstation correlations become less stable, thereby reducing the quality of the dispersion curves and the accuracy of the velocity inversion results [22]. Consequently, the velocity model derived from the ANT method still requires cross-verification with other geophysical methods to ensure its reliability [23].

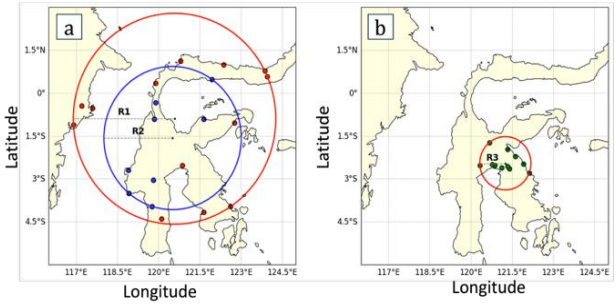

Fig 1: The area of station distribution: (a) previous studies are represented by the red circle (A_1 = 52.54 x 10^4 km^2) [13] and the blue circle (A_2 = 24.21 x 10^4 km^2) [14]; (b) the current study is represented by the red circle (A_3 = 33.49 x 10^2 km^2).

Velocity model plays a crucial role in accurately determining earthquake locations, as they influence the calculation of wave travel times from the source to the recording stations. Global velocity model is often used as a reference, however, this model is generalized and unable to represent regional or local velocity variation that is strongly affected by local geological conditions. This limitation can lead to significant hypocenter location bias, particularly in regions characterized by heterogeneous rock properties in its subsurface [24]. In contrast, local velocity models developed using seismic data from specific regions can better capture both lateral and vertical variations in wave velocity, resulting in more accurate earthquake location determinations [25], [26].

Motivated by the limitations of global velocity models, this research aims to develop a 1-D velocity model along the Matano Fault zone using the VELEST software. We utilized event dataset recorded by 12 permanent stations of BMKG's network distributed around the study area during 2022-2025 period. In general, the 12 stations used were established in 2019, allowing them to record shallow earthquake with small magnitudes. Therefore, for the data used from 2022, the stations were already operating stably.

In addition, four initial velocity models are employed in VELEST to reduce bias. Then, the optimum model is selected based on hypocenter stability and 100 bootstrap analyses. The resulting velocity model is expected to more accurately represent subsurface conditions. Furthermore, this model is expected to be used as a reference for earthquake relocation studies and seismicity analyses along the Matano Fault Zone.

2. Method

The data used in this study include hypocenters, origin times, and P-wave arrival times from earthquakes that occurred within the region bounded by 120.10°E–122.20°E and 2.99°S–1.66°S during the period from January 2022 to March 2025. To ensure the quality of the data analysis, only 317 out of 1,321 earthquake events listed in the BMKG catalog were selected [8]. The selection was based on the criteria of magnitude Mw ≥ 3 and the presence of at least six clearly identified P-wave phases recorded by seismic stations around the Matano Fault. Picking of the P-wave was carried out manually by carefully observing the first impulsive arrival detected on all components. Furthermore, to ensure data quality for subsequent analysis, we initially employed the Wadati Diagram. This method involves plotting the difference between the P-arrival time (TP) and Origin Time (OT) against the difference between the S-arrival time and the P-arrival time for each individual seismic even [27].

Most of the earthquakes in this region are shallow, mainly occuring between 10 and 20 km depth, as shown in Fig. 2. Although there were some non-significant events deeper than 50 km (Fig. 2), we excluded them from the analysis due to poor data quality and unreliable arrival time picks. Therefore

this study focuses on the lithospheric velocity structure down to a maximum depth of 50 km.

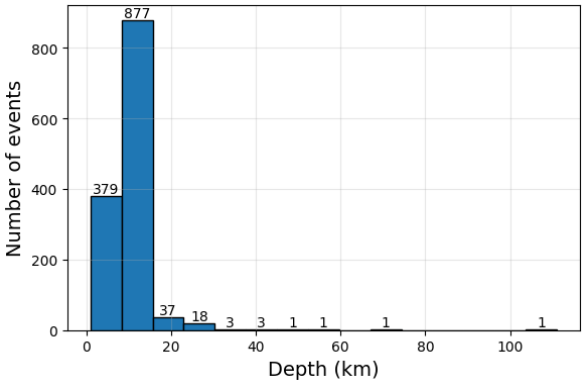

Fig 2: Histogram of earthquake depths.

The optimum 1-D velocity model was obtained through simultaneous inversion of earthquake relocation, seismic velocity, and station corrections using the coupled hypocenter–velocity method implemented in the VELEST program [28]. Although many methods can be used to develop a local velocity model [29, 30], VELEST has the main advantage of efficiency and practicality in using abundant natural earthquake data in tectonically active like the Matano Fault. This program was also applied to develop velocity models for several areas, including along the Western Java Faults, Cimandiri Fault, Lombok Island, Bali, Mamasa, and Mentawai [31, 32, 33, 34, 35, 36, 37].

The VELEST program adopts the principle of the Geiger algorithm, an iterative least-squares approach that calculates hypocenter corrections based on the difference between the observed (t_obs) and theoretical (t_cal) arrival times. During the iterative process, not only the earthquake locations are updated, but the 1-D seismic velocity model is also progressively adjusted until a new velocity model is obtained that more accurately represents the subsurface conditions in the study area. The equation used to determine the travel-time residual (r) is mathematically expressed as:

$$r = t_{obs} - t_{cal} = \sum_{i=1}^{4} \frac{\partial f}{\partial h_i} \Delta h_i + \sum_{j=1}^{n} \frac{\partial f}{\partial v_j} \Delta v_j + \sum_{k=1}^{m} \frac{\partial f}{\partial s_k} \Delta s_k + e \quad (1)$$

where *h, v*, and *s* represent the hypocenter, velocity, and station parameters, respectively, while *Δh, Δv*, and *Δs* denote the changes in the hypocenter, velocity, and station parameters resulting from each iteration. The indices *i, j,* and *k* correspond to the earthquake event, seismic wave velocity at each layer, and station, respectively. Furthermore, m denotes the number of earthquake events, and *n* represents the number of stations.

The initial velocity model plays a crucial function in solving linearized inversion problems [28]. Therefore, this study employed four initial velocity models adapted from previous studies, namely, the Koulakov Model [38], Arimuko Model [39], Crust Model [40], and Bunaga Model [32], as presented in Table 1. This multi-model approach was designed to minimize bias arising from uncertainties in the local subsurface structure and to ensure that the final solution is not only numerically robust but also geologically and seismologically consistent.

Table 1: The initial velocity model for the Koulakov Model [38], Arimuko Model [39], Crust Model [40], and Bunaga Model [32].

Depth (km)	Vp (km/s)			
	Koulakov	Arimuko	Crust	Bunaga
0	4.30	3.78	1.75	4.40
3	4.90	4.34	2.27	5.20
8	5.70	4.90	3.45	6.10
16	6.90	6.84	5.42	5.50
24	7.20	7.52	6.25	7.40
32	7.20	7.52	6.84	7.40
50	7.20	7.52	6.92	7.40

The inversion procedure using VELEST was carried out in three processing stages, as illustrated in Fig. 3. Each s tage employed nine iterations with a damping factor (λ) of 1.0, as recommended by the user manual. The first stage (Run 1) performed hypocenter relocation while simultaneously updating the 1-D velocity model from four initial velocity models. The second stage (Run 2) refined the solution using the hypocenter and velocity model obtained from Run 1, applying the same regularization parameters. A similar procedure was applied in the third stage (Run 3). The optimum model was determined based on a combination of criteria, including the smallest RMS residual, hypocenter stability test [41], bootstrap analysis for uncertainty estimation [42], and consistency with previous studies.

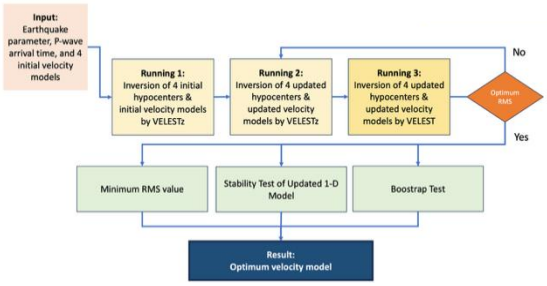

Fig 3: Flowchart of research methodology.

3. Result and Discussion

Seimic activity along strike-slip faults is generally concentrated near the fault line, typically within 4 to 10 km perpendicular distance from the epicenter to the fault line [43]. However, earthquake seismicity along the Matano Fault is distributed up to ~37 km from the fault line, as illustrated in Fig. 4a. The use of a non-optimal velocity model [44] may be one of the factors contributing to the seismicity spreading. Therefore, this study focuses on deriving a local 1-D

velocity model, a relocation of the catalogue using this model is left for future work.

Velocity models that fail to adequately represent local heterogeneity can lead to depth bias. As seen the use of a non-representative velocity model in the BMKG processing system, hypocenters are automatically fixed at a depth of 10 km (Fig. 4b) for earthquakes that are likely to occur at depths of 0–10 km [17]. This study highlights the necessity of updating the velocity model in the Matano Fault area to reduce bias and improve vertical resolution.

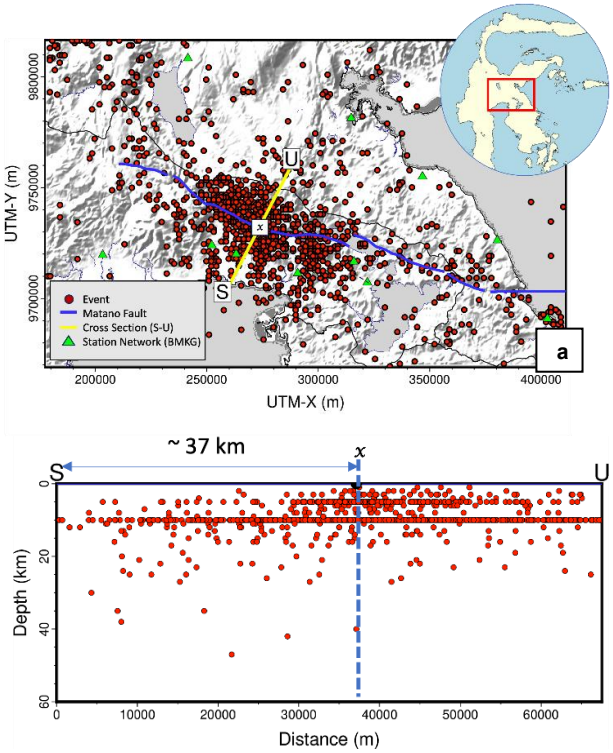

Fig 4: (a) Seismicity of the Matano Fault region from 2022 to 2025 based on the BMKG Catalogue, whereas x indicates the insection between the Matano Fault and the SU cross-section; (b) Earthquake depth profile along the SU cross-section (SW to NE).

Before performing the VELEST inversion, parameterization of the 1-D velocity model is required to ensure that the initial velocity values are properly defined and consistent with region-specific information, such as the Moho depth. This step is crucial because it directly affects the accuracy of the final 1-D velocity model and the precision of subsequent hypocenter determinations [39]. Therefore, the parameterization in this study follows previous studies [32, 38, 39], with an additional layer at the Moho discontinuity from the Central Sulawesi region [45]. The model depth is limited to 50 km, corresponding to the vertical distribution of seismicity along the Matano Fault.

The VELEST inversion for the four initial velocity models was conducted twice, each with up to nine iterations. As shown in Fig. 5, the first inversion produced substantial corrections to the initial models, particularly within the 0–32 km depth range. The second inversion reveals a well-defined low velocity zone (LVZ) at depths of 16–24 km in the Koulakov and Bunaga models. In this depth range, Vp decreases from 6.90 to 4.16 km/s in the Koulakov Model (a reduction of ~40%) and from 5.50 km/s to 4.20 km/s in the Bunaga Model (~24% reduction; Tables 1 and 2). In the case of the Arimuko and Crust Models, LVZ is observed at depths of 24-32 km, whereas Vp decreases from 7.52 to 4.29 km/s in the Arimuko (~43% reduction) Model and 6.25 to 4.27 km/s in the Crust Model (~32% reduction; Tables 1 and 2). Overall, the consistent Vp decrease of approximately 24–43% in the four velocity models indicates the presence of an LVZ within the middle to lower crust beneath the Matano Fault.

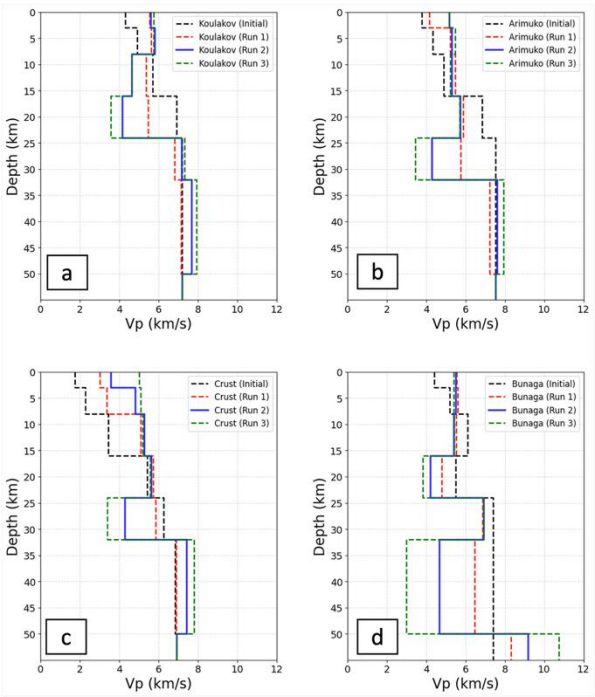

Fig 5: The updated velocity models: (a) The Koulakov Model, (b) The Arimuko Model, (c) The Crust Model, and (d) The Bunaga Model. The black dashed line represents the initial model, the red dashed line shows the updated model after the first run, the blue line shows the updated model after the second run, and the green dashed line shows the updated model after the third run.

Table 2: The updated (Run 2) velocity model in for the Koulakov Model, Arimuko Model, Crust Model, and Bunaga Model.

Depth (km)	Vp (km/s)			
	Koulakov	Arimuko	Crust	Bunaga
0	5.60	5.18	3.57	5.50
3	5.79	5.30	4.80	5.50
8	4.63	5.30	5.27	5.41
16	4.16	5.72	5.61	4.20
24	7.17	4.29	4.27	6.91
32	7.66	7.60	7.41	4.66
50	7.20	7.52	6.92	9.17

The LVZ indicates a layer of relatively weak or less compact rock, which may be associated with the occurrence of unconsolidated sedimentary rocks

such as clay, silt, and loose sand [46]. In this study, the presence of the LVZ in the Matano Fault is suspected to be linked to the rapid uplift of Central Sulawesi. This uplift was initially triggered by the collision between East and West Sulawesi that occurred following the accretion of the East Sulawesi Ophiolite in the late Oligocene. The uplift then continued and was accelerated by a transpressional regime (a combination of compression and shear stress) active between 5 and 2 million years ago. This uplift process and the region's tropical latitude caused very high erosion rates, which indirectly resulted in the formation of thick, unconsolidated sedimentary packages filling the extension zone [45].

The occurrence of an LVZ extending to certain depths suggests the presence of thick sedimentary layers, where greater sediment thickness corresponds to lower seismic wave velocities. This condition reflects a significant sediment accumulation zone formed by rapid uplift, intense erosion, and continuous deposition within the basin area [20]. In addition, low-velocity characteristics may also indicate the presence of weathered volcanic rocks or fractured zones, such as tuff, volcanic breccia, and altered lava, which are commonly found in active volcanic or volcano-tectonic regions [47]. Another possible type is rock containing fluids or partial melts, such as basalt and andesite at intermediate depths, which may contain partially molten magma and are often interpreted as magma storage zones or partial melt zones.

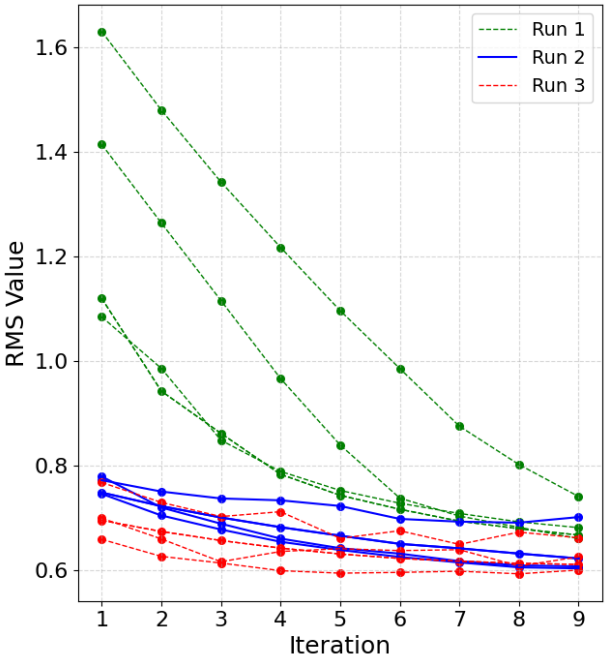

Fig 6: The RMS values for each iteration across all models and processing runs (Run 1-3). The green dashed lines represent Run 1 for Kolakov, Arimuko, Crust, and Bunaga Models, while the blue dashed lines represent Run 2 and the red dashed lines represent Run 3.

Based on the Root Mean Square (RMS) values, the inversion results from the three processing stages show a decreasing trend in RMS with each iteration (Fig. 6). This indicates an improvement in the fit between the observed data and the model calculations as the inversion process progresses. The most significant RMS reduction occurred in Run 1, where the initial value of approximately 1.6 sharply decreased to around 0.8 by the ninth iteration. In Run 2, the RMS decrease was relatively smaller but still showed a steady improvement, reaching about 0.65. Meanwhile, Run 3 exhibited an RMS value that was nearly convergent from the early iterations, with only minor reductions after the fifth iteration.

A detailed comparison of Run 1 and Run 2 (Fig. 7) reveals distinct performance characteristics among the initial models. The Crust model (black dashed line) exhibits the highest initial RMS (>1.6 s) and requires the most significant adjustment, reflecting its nature as a global model far from local conditions. In contrast, the Bunaga model (green) demonstrates the most efficient performance. It starts with a low RMS in Run 1 and rapidly stabilizes at the lowest residual level (~0.62 s) in Run 2, suggesting that its vertical gradient offers the closest approximation to the study area's specific velocity structure.

Meanwhile, the Koulakov model (blue) shows a moderate convergence rate, stabilizing at a slightly higher RMS (~0.70 s) in Run 2 compared to the other models. This result implies that while the Koulakov model is robust (stable), it yields a slightly higher data misfit compared to the Bunaga or Arimuko models. This phenomenon is consistent with the general principles of geophysical inversion, where the degree of similarity between the initial model and the actual geological conditions directly affects the convergence limit [48]. Consequently, the lower final RMS of the Bunaga and Arimuko models demonstrates a closer quantitative agreement with the observational data.

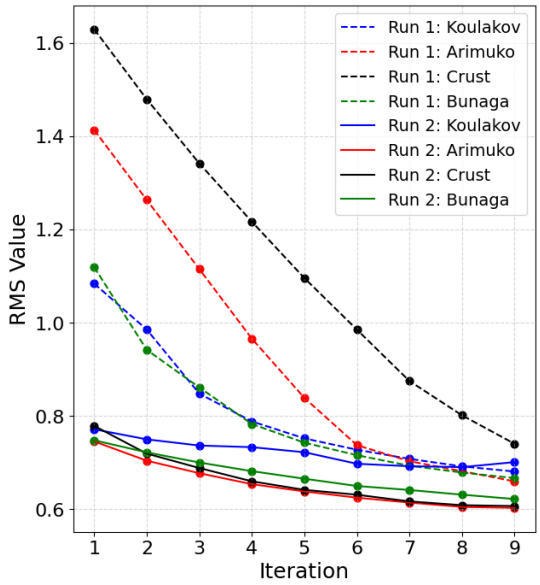

Fig 7: Comparison of the RMS values for Run 1 and Run 2 across all models.

Fig. 8 presents a comparison of RMS values between Run 2 and Run 3 for the four velocity models. In general, all models exhibit a consistent decreasing

trend in RMS values with increasing iterations. Interestingly, in Run 3, fluctuations in convergence are observed in the Koulakov, Arimuko, and Crust models, characterized by the appearance of several local minimum RMS values. This phenomenon is a consequence of the non-linear nature of local earthquake inversion, where the interaction between the velocity model, hypocenter locations, and station corrections can produce multiple local solutions with minimum RMS values [28]. Therefore, the fluctuating pattern observed in Run 3 indicates that the inversion process is still in the stage of seeking equilibrium, whereas Run 2 shows a more stable and consistent RMS reduction pattern.

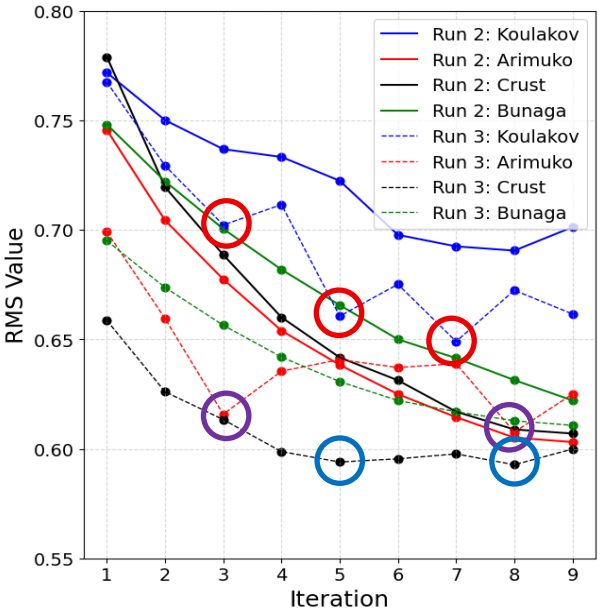

Fig 8: Comparison of the RMS values for Run 2 and Run 3 across all models. The red, purple, and blue circles indicate several local minima of RMS value for the Koulakov, Arimuko, and Crust Models (Run 3), respectively.

Based on Fig. 9, the inversion results from the second stage (Run 2) show the best performance compared to the first and third inversion stages. This is indicated by the optimum ("best-fit") RMS value achieved at the 8th iteration, representing the best balance point between the velocity model and the observational data. Therefore, the inversion results from this stage can be considered the most representative for the study area. Furthermore, the Arimuko model demonstrates the most optimal result, characterized by the lowest optimum RMS value among all velocity models, indicating a better agreement between the velocity model and the actual subsurface conditions.

The next evaluation after examining the RMS values is the stability test, which aims to determine the most stable 1-D velocity model (Run 2) and to identify potential biases in hypocenter locations. This test is performed by introducing perturbations to the hypocenter positions, either randomly or systematically

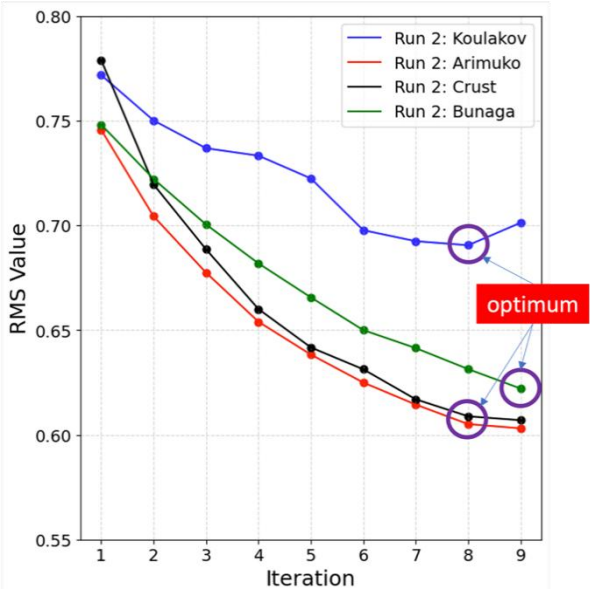

Fig 9: The final RMS result for each iteration across all models. The purple circle indicates an optimum (or "best fit") solution at this study area.

All hypocenters are shifted in all directions by approximately 6–7 km using a Gaussian distribution with a mean value of zero, resulting in random and patternless variations [41]. The inversion process is then repeated to obtain new hypocenter locations. The 1-D velocity model can be considered stable if the inverted hypocenters do not show significant changes compared to the original ones [41, 42]. This condition is indicated by hypocenter shifts approaching zero, as shown in red in Fig. 10.

The next evaluation, following the examination of RMS values, involves a stability test to determine the most stable 1-D velocity model (Run 2) and to identify potential biases in hypocenter locations. This test is conducted by introducing perturbations to the hypocenter positions, both randomly and systematically. All hypocenters are shifted in all directions by approximately 6–7 km using a Gaussian distribution with a mean of zero, resulting in random variations with no systematic pattern [26]. The inversion process is then repeated to obtain new hypocenter locations. The 1-D velocity model can be considered stable if the relocated hypocenters do not exhibit significant changes compared to the original ones [41, 42]. This condition is indicated by hypocenter shifts approaching zero, as shown in red in Fig. 10.

Fig. 10 illustrates the results of the stability test for the 1-D velocity models obtained from the second inversion stage. Based on these results, the Arimuko model exhibits the highest stability, as it shows a balanced distribution of hypocenter shifts—neither as extreme as in the Koulakov and Crust models nor as rigid toward data variations as the Bunaga model. However, the depth parameter still displays an unstable pattern across all models, indicating that vertical stability of the hypocenters has not been fully achieved.

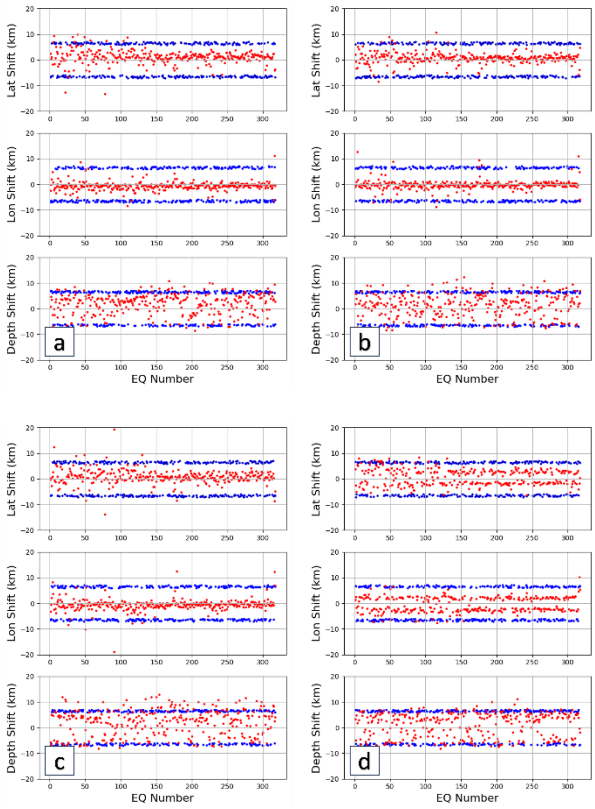

Fig 10: The stability test results of the 1-D velocity model from the second inversion (Run 2): (a) The Koulakov Model, (b) The Arimuko Model, (c) The Crust Model, and (d) The Bunaga Model. The blue dots represent the initial hypocenter positions before inversion, while the red dots indicate the relocated hypocenters after inversion, which have shifted back toward their original positions (prior to the applied perturbation).

The current level of computational capacity enables the implementation of various statistical tests that consider the influence of uncertainties in hypocenter locations and initial velocity models on the inversion results. Nevertheless, the limited amount of data contributes significantly to the level of model uncertainty, thereby affecting the reliability of the inversion outcomes. As in most statistical problems, the reliability of the model produced through inversion increases with the amount of data used. This is due to the inverse relationship between the standard deviation of model parameters and the data quantity, where a larger dataset results in lower standard deviation values [42].

One of the most effective methods currently used to assess uncertainty due to data limitations is the bootstrap or resampling method. The bootstrap method works by generating new datasets through random sampling from the existing dataset. This sampling process follows a "sampling with replacement" scheme, meaning that data elements already selected remain in the original dataset and can be chosen repeatedly [47]. Resampling methods such as bootstrap offer significant advantages over conventional approaches.

In this study, the bootstrap process was performed 100 times using 159 out of a total of 317 earthquake events selected randomly. The bootstrap test results (Fig. 11) indicate that the Arimuko model exhibits the tightest and most homogeneous distribution of bootstrap outcomes, from the surface down to a depth of approximately 25 km, among the four models tested. This suggests that the velocity variations among the bootstrap samples are minimal, indicating that this model can be classified as stable and consistent within the upper crustal layer. Furthermore, the comparison between the average velocity model and the Run 2 velocity model (in red) shows good agreement, with no significant shifts in the position of the velocity layers.

Further statistical analysis of the standard deviation for each model (Fig. 12) reinforces these findings. The standard deviation values of the Arimuko model are generally lower than those of the other models, particularly at depths of 0–25 km. These low deviation values indicate that the inversion results of the Arimuko model are relatively insensitive to variations in input data and, therefore, exhibit a higher level of reliability.

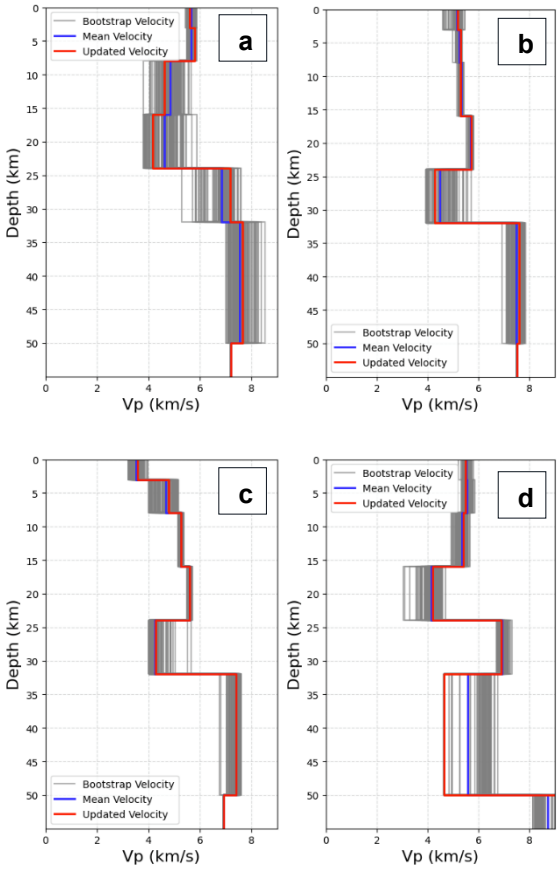

Fig 11: The bootsratp results of the 1-D velocity model from the second inversion (Run 2): (a) The Koulakov Model (b) The Arimuko Model, (c) The Crust Model, and (d) The Bunaga Model.

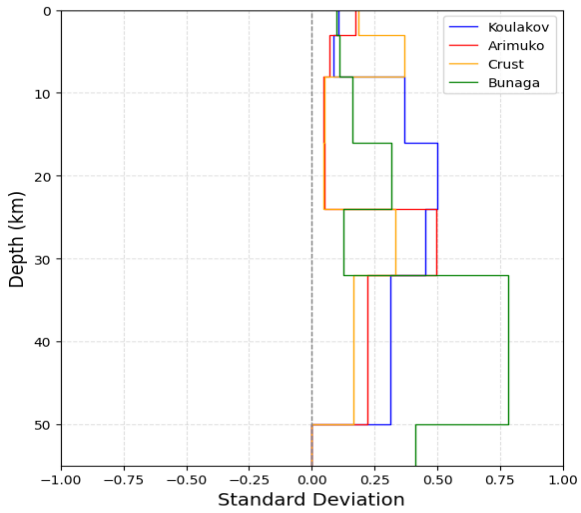

Fig 12: Standard deviation for all models.

4. Conclusion

Based on the evaluations conducted, including RMS analysis, model stability testing, and bootstrap assessment, it can be concluded that the Arimuko model consistently demonstrates the best performance among the four models tested. This model produces relatively low RMS values, exhibits the highest stable inversion results across all models, and shows tightly clustered bootstrap distributions with the lowest standard deviation values. These findings indicate that the Arimuko model is the most stable, reliable, and representative velocity model for characterizing the subsurface structure in the study area.

Acknowledgment

The authors wish to express their sincere appreciation to Dr. Nelly Florida Riama, Deputy for Geophysics, for her valuable support and the financial assistance that made this research possible.

References

[1] M. R. Daryono, B. Kumarawarman, I. H. Muslim, Rr. Triwurjani, R. Permadi, S. Prihatmoko, S. Wibowo, and G. H. Tutuko, "Two Earthquake Events on the Pamsoa Segment of the Matano Fault, Sulawesi" IOP Conf. Ser.: Earth Environ. Sci., 873(1),012053, (2021).

[2] A. Khairi, M. Awaluddin, and B. Sudarsono, "Analisis Deformasi Seismik Sesar Matano Menggunakan GNSS dan Interferometrik SAR" J. Geodesi Undip, 9(2),32–42, (2020).

[3] Pusat Studi Gempa Nasional (Indonesia), Peta Sumber dan Bahaya Gempa Indonesia Tahun 2017, Pusat Penelitian dan Pengembangan Perumahan dan Permukiman, Badan Penelitian dan Pengembangan, Kementerian Pekerjaan Umum, (2017).

[4] A. Patria, D. H. Natawidjaja, M. R. Daryono, M. Hanif, A. R. Puji, and H. Tsutsumi, "Tectonic Landform and Paleoseismic Events of the Easternmost Matano Fault in Sulawesi, Indonesia" Tectonophysics, 852, 229762, (2023).

[5] A. Walpersdorf, C. Vigny, C. Subarya, and P. Manurung, "Monitoring of the Palu-Koro Fault (Sulawesi) by GPS" Geophys. Res. Lett., 25(13), 2313–2316, (1998).

[6] A. Socquet, W. Simons, C. Vigny, R. McCaffrey, C. Subarya, D. Sarsito, B. Ambrosius, and W. Spakman, "Microblock Rotations and Fault Coupling in SE Asia Triple Junction (Sulawesi, Indonesia) from GPS and Earthquake Slip Vector Data" J. Geophys. Res.: Solid Earth, 111(B8), 1–15, (2006).

[7] The Indonesian Agency for Meteorolgy, Climatology, and Geophysics, Jakarta, Indonesia, "Laporan Tahunan BMKG 2017" (2017).

[8] The Indonesian Agency for Meteorolgy, Climatology, and Geophysics, Jakarta, Indonesia", "InaTEWS Earthquake Repository," (2022).

[9] M. R. Daryono, "Paleoseismology of Tropical Indonesia (Case Study in Sumatran Fault, Palukoro-Matano Fault, and Lembang Fault) (Paleoseismologi Tropis Indonesia (Dengan Studi Kasus di Sesar Sumatra, Sesar Palukoro-Matano, dan Sesar Lembang))," Doctoral Dissertation, Institut Teknologi Bandung, (2016).

[10] A. Cipta, R. Robiana, J. D. Griffin, N. Horspool, S. Hidayati, and P. R. Cummins, "A probabilistic seismic hazard assessment for Sulawesi, Indonesia," 441, 133–152, (2017).

[11] I. M. Watkinson and R. Hall, "Tectonic Fault Systems at The Triple Junction of Eastern Indonesia: Evaluation of Quaternary Activity and Implications for Seismic Hazard" Geol. Soc. Spec. Publ., 441, (2017).

[12] Muh. Karnaen, “Studi Kerentanan Bencana Gempa Bumi di Sekitar Sesar Matano,” IOP Conf. Serr.: Earth Environ. Sci., 235, 011001, (2019).

[13] H. Permana and Surono, Geologi Sulawesi: Kompleks Ofiolit, Bandung: LIPI Press, (2015).

[14] D. A. Suriamihardja, M Karnean, A. Maulana, and A. Jaya, "Study of Correlation Between Rock Type and B-Value on Seismic Characteristics of Matano Fault" Int. J. Earth Sci. Eng., 11(2), 153–158, (2018).

[15] D. Kusumawati, D. P. Sahara, N. T. Puspito, A. W. Baskara, A. Kurniawan, W. Tanihaha, L. Junior, J. Solihin, M. D. Pratama, S. H. Patimah, A. T. Sasmi, H. Muhammad, H. Muhammad , W. C. Natafrisca, and M. A. Bening, "Moment Tensor Inversion Implementation in Determining Focal Mechanism Solution of Palu-Koro and Matano Fault Events: Processing Strategy" In IOP Conf. Ser.: Earth Environ. Sci., 1227(1), 012043, (2023).

[16] P. Supendi N. Rawlinson, J. Han, S. Widiyantoro, S. Pilia, A. D. Nugraha, and D. Karnawati, "Evidence of Magma Reservoirs Beneath Volcanoes in Northern Sulawesi and The Molucca Sea from Regional Earthquake Tomography" Geophys. Res. Lett., 52(3), 1–9, (2025).

[17] L. N. Azizah, A. Tjahjono, and A. Sabtaji, "Relokasi Hiposenter Gempa Bumi dan Model Struktur

Kecepatan 1 Dimensi Gelombang P dengan Menggunakan Metode Coupled Velocity–Hypocenter di Daerah Sulawesi Tengah dan Sekitarnya" Al-Fiziya: J. Materials Sci., Geophysics, Instrumentation & Theoretical Phys., 2(1), 1–9, (2019).
[18] K. Azizah, A. Susilo, and T. D. Rachman, "Studi Relokasi Hiposenter Gempa di Sekitar Patahan Palu Koro dan Matano Menggunakan Metode Geiger" Brawijaya Phys. Student J., 2 (1), 1–4, (2014).
[19] M. S. Rosid, Y. H. Ali, and M. Ramdhan, "Characterization of the Mamasa Earthquake Source Based on Hypocenter Relocation and Gravity Derivative Data Analysis" GEOMATE Journal, 23 (97), 220–227, (2022).
[20] N. Heryandoko, A. D. Nugraha, Z. Zulfakriza, S. Rosalia, T. Yudistira, S. Rohadi, D. Daryono, and S. Widiyantoro, "Crustal Thickness Variation of Kalimantan and Sulawesi Region from Teleseismic Receiver Function" Journal of Seismology, 28 (3), 879–898, (2024).
[21] S. Noi, A. Taufiq, A. Amiruddin, and D. A. Zaky, "Ambient Seismic Noise Tomography Imaging of The Etna Volcanic Complex in Italy" IOP Conf. Ser.: Earth and Environmental Science, vol. 1521(1), 012018, (2025).
[22] Y. Yang and M. H. Ritzwoller, "Characteristics of Ambient Seismic Noise as a Source for Surface Wave Tomography" Geochemistry, Geophysics, Geosystems, 9(2), 1-18 (2008).
[23] E. D. Kästle, A. El-Sharkawy, L. Boschi, T. Meier, C. Rosenberg, N. Bellahsen, L. Cristianoand C. Weidle, "Surface Wave Tomography of the Alps Using Ambient-Noise and Earthquake Phase Velocity Measurements" J. Geophys. Res.: Solid Earth, 123(2), 1770–1792, (2018)
[24] N. Asra and U. Muksin, "The Effect of Velocity Model to Local Earthquake Location" AIP Conf. Proc., 3082(1), 030020, (2024).
[25] F. Waldhauser and W. L. Ellsworth, "A Double-Difference Earthquake Location Algorithm" Bull. Seismol. Soc. Am., vol. 90(6), 1353–1368, (2000).
[26] M. S. Rosid, I.G. K. S. Bunaga, T. Anggono, G. Daniarsyad, A. Arimuko, M. Najib, Y. Setiawan, D. Sianipar, A. Septiadhi, S.P. Adi and D. Akbar," The 2019 Mw 5.4 East Lombok Earthquake: A Shallow Fault Reactivation" J. Volcanol. Seismol., 19, 397–409, (2025).
[27] K. Wadati and S. Oki, "On the Travel Time of Earthquake Waves (Part II)" J. Meteorol. Soc. Jpn., 11(1), 14–28, (1933).
[28] E. Kissling, U. Kradolfer, and H. Maurer, "Program VELEST User's Guide—Short Introduction" Institute of Geophysics, ETH Zurich, 22, (1995).
[29] E. M. Syracuse, H. Zhang, and M. Maceira, "Joint Inversion of Seismic and Gravity Data for Imaging Seismic Velocity Structure of the Crust and Upper Mantle Beneath Utah, United States" Tectonophysics, 718, 105–117, (2017).
[30] R. Movaghari and G. Javan Doloei, "3-D Crustal Structure of the Iran Plateau Using Phase Velocity Ambient Noise Tomography" Geophys. J. Int., 220(3), 1555–1568 (2020).
[31] N. Sari, M. S. Rosid and T. Anggono, "Relokasi Hiposenter Double Difference dan Penentuan Model Kecepatan di Jawa Bagian Barat Tahun 2010–2024 untuk Identifikasi Patahan" POSITRON, 15(1), 81–93, (2025).
[32] I. G. K. S. Bunaga, M. S. Rosid, T. Anggono, and A. Septiadhi, "Determination of 1-D Seismic Velocity Model in Lombok Island" J. Penelit. Pendidikan IPA, vol. 9(12), 10663–10670, (2023).
[33] Pepen Supendi, A. D. Nugraha, S. Widiyantoro, C. I. Abdullah, N. T. Puspito, K. H. Palgunadi, D. Daryono, and S. H. Wiyono, "Hypocenter Relocation of the Aftershocks of the Mw 7.5 Palu Earthquake (September 28, 2018) and swarm Earthquakes of Mamasa, Sulawesi, Indonesia, Using the BMKG Network Data" Geoscience Lett., 6(1), 18, (2019).
[34] D. P. Sahara, P. P. Rahsetyo, A. D. Nugraha, D. K. Syahbana, S. Widiyantoro, Z. Zulfakriza, A. Ardianto, A. W. Baskara, S. Rosalia, M. Martanto, and H. Afif, "Use of Local Seismic Network in Analysis of Volcano-Tectonic (VT) Events Preceding the 2017 Agung Volcano Eruption (Bali, Indonesia)" Front. Earth Sci., 9, 619801, (2021).
[35] M. Ramdhan, S. Widiyantoro, A. D. Nugraha, J.-P. Métaxian, A. Saepuloh, S. Kristyawan, A. S. Sembiring, A. B. Santoso, A. Laurin, and A. A. Fahmi, "Relocation of Hypocenters From DOMERAPI and BMKG Networks: A Preliminary Result From DOMERAPI Project" Earthquake Sci.,30(2), 67–79, (2017).
[36] S. H. Maulani, R. Refrizon, R. Samdara, L. A. Satria, and S. Ahadi, "Relocation of the Hypocenter of an Earthquake with the Double Difference Method in the Mentawai" J. Geocelebes,9(2), 126–138, (2025).
[37] P. Supendi and A. D. Nugraha, "Preliminary Result of Earthquake Hypocenter Determination Using Hypoellipse around Western Java Region" In AIP Conf. Proc., 1730 (1),020002, (2016).
[38] I. Koulakov, A. Jakovlev, and B. G. Luehr, "Anisotropic Structure Beneath Central Java from Local Earthquake Tomography" Geochem. Geophys. Geosyst.,10(2), Q02011, (2009).
[39] A. Arimuko, B. M. Nanda, and R. Rasmid, "Identifikasi Struktur Bawah Permukaan Berdasarkan Pemodelan Kecepatan 1D Hasil Relokasi Hiposentrum Gempa di Pulau Lombok, Gunung Sinabung, dan Jailolo" J. Geofis.,18(2),40–48, (2020).
[40] G. Laske, G. Masters, Z. Ma, and M. Pasyanos, "Update on CRUST1.0—A 1-Degree Global Model of Earth's Crust" Geophys. Res. Abstr.,15(15), 2658, (2013).
[41] M. F. Akkoyunlu, B. Kaypak, B. Oruç, and D. Kalafat, "Derivation of A 1-D Seismic Velocity

Model for The Lake Van Region" Turk. J. Earth Sci., 33(4), 407–429, (2024).
[42] H. Langer, R. Raffaele, A. Scaltrito, and L. Scarfi, "Estimation Of An Optimum Velocity Model In The Calabro-Peloritan Mountains—Assessment Of The Variance Of Model Parameters And Variability Of Earthquake Locations" Geophys. J. Int., 170(3), 1151–1164, (2007).
[43] P. M. Powers and T. H. Jordan, "Distribution Of Seismicity Across Strike-Slip Faults In California" J. Geophys. Res.: Solid Earth, 115(B5), 1–25, (2010).
[44] S. Husen, E. Kissling, N. Deichmann, S. Wiemer, D. Giardini, and M. Baer, "Probabilistic Earthquake Location in Complex Three-Dimensional Velocity Models: Application to Switzerland" J. Geophys. Res.: Solid Earth, 108(B2), 2077, (2003).
[45] N. Rawlinson, S. Pozgay, and S. Fishwick, "Seismic Tomography: A Window into Deep Earth" Physics of the Earth and Planetary Interiors, 178(3–4), 101–135, (2010).
[46] P. Kearey, M. Brooks, and I. Hill, An Introduction to Geophysical Exploration, 3rd ed., Oxford: Blackwell Science Ltd., (2002).
[47] V. Lyakhovsky, E. Shalev, I. Kurzon, W. Zhu, L. Montesi, and N. M. Shapiro, "Kecepatan dan Redaman Gelombang Seismik Efektif pada Batuan yang Sebagian Meleleh" Earth Planet. Sci. Lett., 572, 117117, (2021).
[48] N. Heryandoko, D. Nugraha, Z. Zulfakriza, S. Rosalia, T. Yudistira, S. Rohadi, D. Daryono, P. Supendi, N. Nurpujiono, F. Yusuf, F. Fauzi, A. Lesmana, Y. M. Husni, B. S. Prayitno, R. Triyono, S. P. Adi, D. Karnawati, T. Greenfield, N. Rawlinson, and S. Widiyantoro, "Struktur Kerak Kalimantan, Selat Makassar dan Sulawesi dari Tomografi Kebisingan Sekitar" Jurnal Geofisika Internasional, 237(2), 949–964, (2024).